

${}^9\text{B}$ excited states and analysis of the ${}^9\text{Be}({}^3\text{He},t)$ spectra

K. Kadija, G. Paić, and B. Antolković
Rudjer Bošković Institute, 41001 Zagreb, Yugoslavia

A. Djalois and J. Bojowald
Institut für Kernphysik, Kernforschungsanlage Jülich, D-5170 Jülich, Federal Republic of Germany
 (Received 25 July 1986; revised manuscript received 11 February 1987)

Inclusive spectra of $({}^3\text{He},t)$ on ${}^9\text{Be}$ have been measured and analyzed in a large energy range of emitted tritons at $E_{3\text{He}}=90$ MeV in the angular range 7° – 27° . The spectra have been analyzed in terms of a superposition of simultaneous breakups, quasifree reactions, and two-step-fragmentation plus pickup processes. The residual spectra correspond to excited states in ${}^9\text{B}$. Confirmation for uncertain states was obtained. Some new states, possible analogs to ${}^9\text{Be}$, were observed.

I. INTRODUCTION

The study of the $({}^3\text{He},t)$ reaction was initiated by the following considerations.

(i) The $({}^3\text{He},t)$ reaction is a useful tool for the analysis of isospin analog states in mirror nuclei. In Fig. 1 we show the latest level structure of ${}^9\text{Be}$ and ${}^9\text{B}$.¹ One sees that still several levels observed in ${}^9\text{Be}$ have not been reported in ${}^9\text{B}$.

(ii) In $({}^3\text{He},t)$ reactions large structures have been observed at $\sim \frac{2}{3}$ the incident energy of the ${}^3\text{He}$ particles.^{2,3} The observations were made for medium heavy nuclei for ${}^3\text{He}$ energies of 90 and 130 MeV, and the data were interpreted as the result of a two step process in which the first step belongs to the fragmentation of the incident ${}^3\text{He}$, and the second step to the pickup of a neutron by the deuteron fragment.^{2,3} The use of a light target where only a few final states can be reached via the proposed mechanism seems indicated to learn more about the processes involved.

II. EXPERIMENT

The experiment was performed using the 90 MeV ${}^3\text{He}$ beams from the isochronous cyclotron JULIC. Depending on the measuring angle beam intensities in the range 10–50 nA kept the dead time to a negligible level. The target was a 2.7 mg/cm² foil of beryllium. The charged reaction products were detected by a ΔE - E telescope inside a 1 m scattering chamber. The ΔE counter was a commercial Si surface barrier detector 400 μm thick. A side entry 31 mm thick Ge(Li) detector mounted in a separate cryostat⁴ served as an E counter. Coincident signals from the ΔE and E counters of each telescope were fed separately, via standard electronics, into an ND 6660 multichannel analyzer where particle identification was performed and energy spectra for various outgoing charged particle types were produced. At the end of each run, the spectra were written onto a magnetic tape for off line analysis. A Ge(Li) detector situated at a fixed angle of $\theta_{\text{lab}} = -30^\circ$ served as a monitor. Measurements were taken at 7° , 10° , 15° , 21° and 27° .

III. ANALYSIS OF SPECTRA

The spectra at forward angle revealed upon analysis that, besides the excitation of the states of the residual ${}^9\text{B}$ nucleus, one may distinguish three additional contributions.

(i) A part proportional to a linear combination of phase spaces (PS) as observed in several works.^{5–7}

(ii) The structure observed earlier by Ref. 2 located at $\sim \frac{2}{3}$ of the incident energy and attributed to the two step process (TSP).

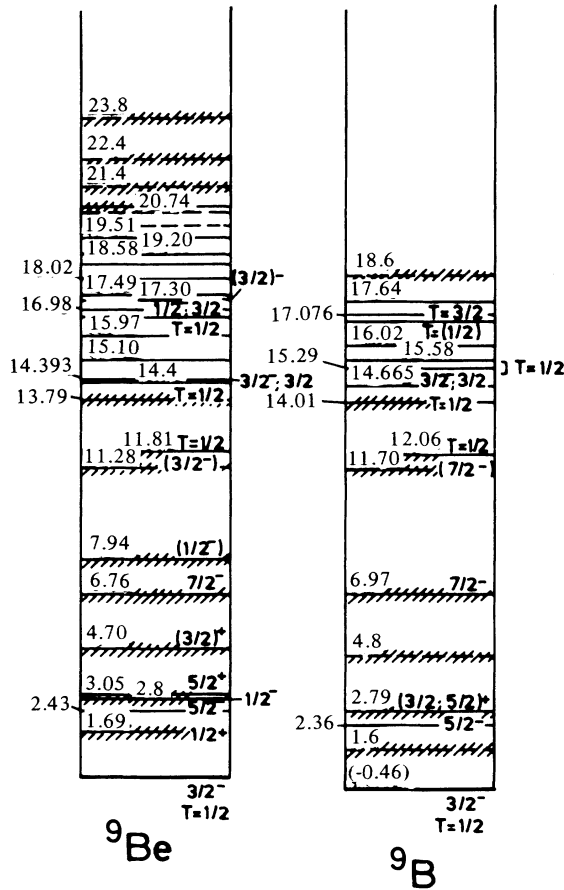
(iii) A prominent large peak corresponding to the quasifree $({}^3\text{He},t)$ reaction (QFR) on the ${}^5\text{He}$ cluster in ${}^9\text{Be}$.

The simultaneous fit to all the excited states and the processes (i) to (iii) was not practical and would be too ambiguous. We have therefore proceeded by successive strippings of all the processes underlying the excited states.

A. Analysis of the (PS)

We used at all angles a linear combination of the following final channels: $(t, {}^8\text{Be}, p)$ and (t, α, p, α) . Amplitudes of individual phase space distributions were fixed by fitting only the low energy part of the spectrum where interferences from recognizable structures (like TSP) in the spectra are negligible. Figure 2 shows the (PS) contribution to a representative spectrum. The differential cross sections of individual final channels obtained following the formulae in Ref. 7 are given in Fig. 3.

The interesting result from the present analysis is that, contrary to the experience in fitting inclusive spectra of the breakups induced by other particles (p and α), the breakups which differ from the most obvious configurations $(t, {}^8\text{Be}, p)$ and (t, α, α, p) are nonexistent. In addition, the angular distribution confirms the earlier reported fact that at low angles the three body breakup contribution is dominant. This result is in contradiction with the findings of Ueno *et al.*⁸ for the same reaction

FIG. 1. Level scheme of ${}^9\text{Be}$ and ${}^9\text{B}$ after Ref. 1.

measured at 6.7 MeV; they find a dominant contribution of four body breakup. However, the Coulomb correction introduced in their analysis is questionable and may have led the authors to wrong conclusions. Specifically, the correction used favors the emission of high triton momenta corresponding to low relative momenta among the constituents of the unstable ${}^9\text{B}$. However, they did

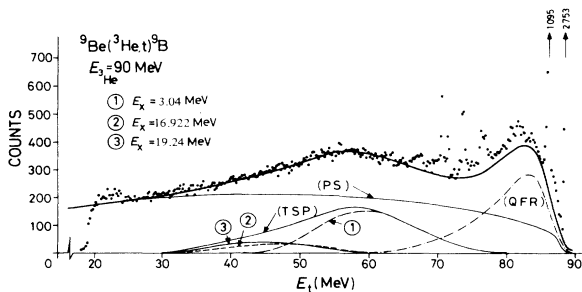


FIG. 2. Inclusive experimental triton spectrum measured at 7° (dots). The heavy solid line indicates the total fit to the continuous part of the spectrum obtained by incoherent summation of the phase space (PS) component, a two step process (TSP) component which is the sum of contributions 1, 2, and 3 involving the 3.04, 16.922, and 19.24 MeV state in ${}^8\text{Be}$, respectively, and a quasifree reaction (QFR) component (dashed-dotted line).

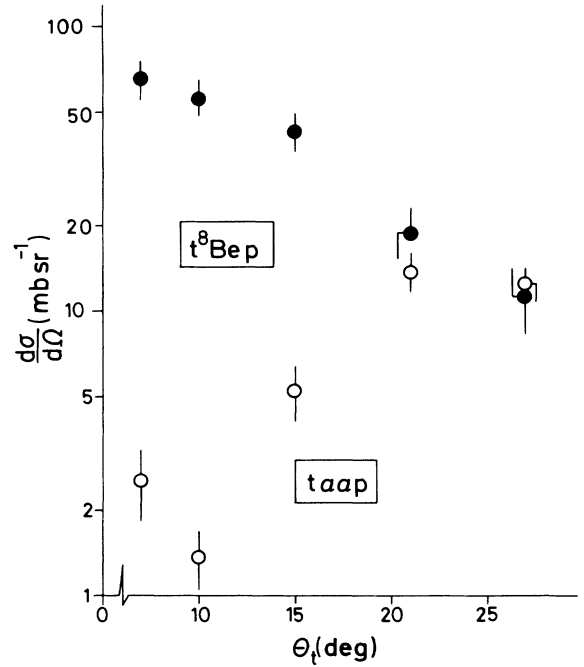


FIG. 3. Angular distribution of the two calculated final state elements contributing to the phase space (PS) component.

not take into account that the Coulomb repulsion among these constituents hinders the emission of tritons with high momenta.

B. Analysis of the (TSP)

After we stripped off the (PS) contribution, the shape of the spectra was recalculated along the lines of Serber's model⁹ by introducing the following assumptions.

(a) The (d,t) reactions leading to the 3.04, 16.922, and 19.24 MeV states in ${}^8\text{Be}$ have been considered [in agreement with the results of the ${}^9\text{Be}$ (d,t) reaction measured at the almost corresponding energy¹⁰].

(b) The cross section for the (d,t) reaction was constant for the whole range of incident deuterons.

(c) The differential cross section is strongly forward peaked and the angular distribution of the (d,t) reaction shall not significantly distort the spectra.

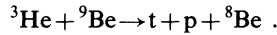
(d) Only deuterons that have been spectators throughout the breakup of ${}^3\text{He}$ in the field of ${}^9\text{Be}$ have been considered in the calculations.

The first part of the process, i.e., the breakup of the ${}^3\text{He}$ is calculated in the framework of Serber's model using the relation

$$\frac{d^2\sigma}{d\Omega_t dE_t} = \sum_{i=1}^3 C_i |G(p)|^2 R_2^*(m_p, m_{8\text{Be}}^i, E - E_t, \mathbf{P} - \mathbf{p}_t), \quad (1)$$

where C_i is a normalization factor; R_2^* is the phase space factor; m_p and $m_{8\text{Be}}^i$ are the masses of the proton and ${}^8\text{Be}$ in a given state i , respectively; E and \mathbf{P} are the

total energy and momentum in the reaction



The index i denotes the final state of the ${}^8\text{Be}$ nucleus considered; E_t and p_t are the energy and momentum of the detected triton, respectively. For the wave function of the relative motion of the proton and deuteron in ${}^3\text{He}$ we used the Yukawa form¹¹

$$\Psi_{{}^3\text{He}}(r) = C' \left[\frac{\alpha}{2\pi} \right] \frac{1}{r} e^{-\alpha r} \quad (2)$$

with

$$\alpha = \frac{(2\mu\epsilon_{{}^3\text{He}})^{1/2}}{\hbar}, \quad (3)$$

where μ is the reduced mass, $\epsilon_{{}^3\text{He}}$ the separation energy of the proton from ${}^3\text{He}$, and C' is a normalization constant. The Fourier transform has been calculated using a cutoff in the spatial wave function as a fitting parameter. The cutoff radius was introduced to simulate the effect of the solid angle of the detector on different momentum components of the Fourier transform. This correction is not the same at all angles and therefore, the

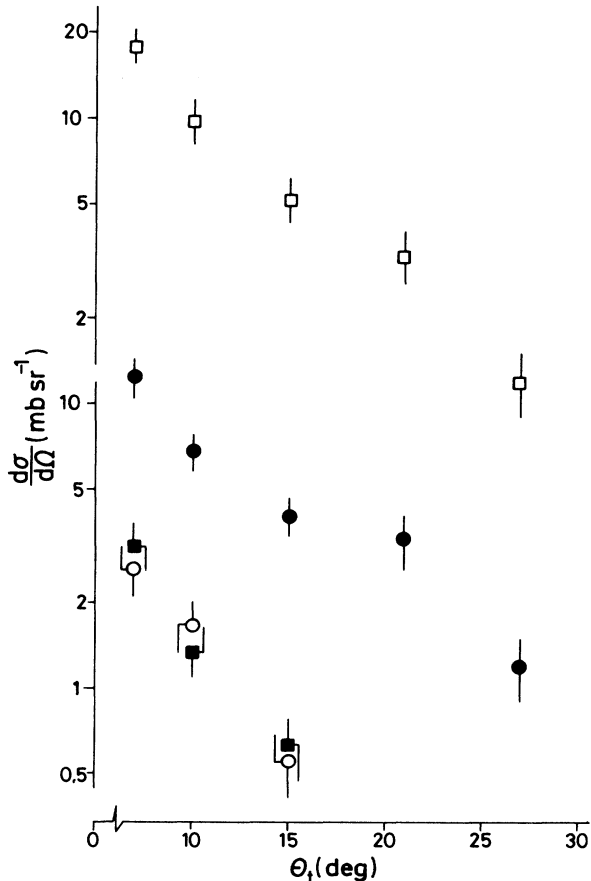


FIG. 4. Angular distribution of the estimated total two step process (TSP) component (open squares) and the individual transitions to the 3.04 MeV (solid circles), 16.922 MeV (open circles), and 19.24 MeV (solid squares) states of ${}^8\text{Be}$.

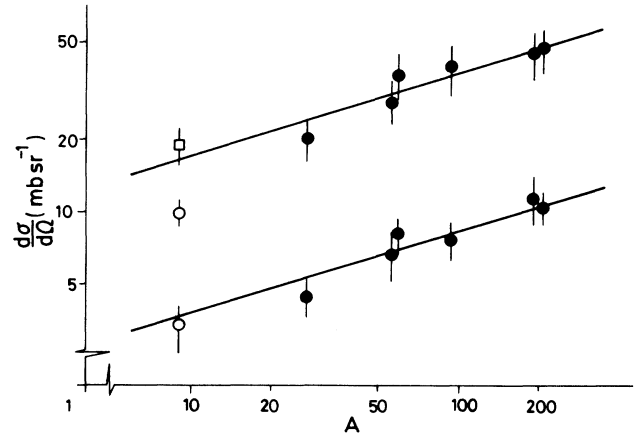


FIG. 5. A dependence of the two step process (TSP) component from Ref. 2 at 12° (upper points) and 22° (lower points) completed with our data at 10° and 21° (open circles). The open square indicates the result obtained if a linear background is assumed at 10° . The solid lines indicate the $A^{1/3}$ behavior.

cutoff radius decreases with angle. In addition, the introduction of the cutoff simulates effects of the details of the process not taken into account by the present model. The angular variation of the cross section extracted from the present analysis is shown in Fig. 4. In Fig. 2 the contribution of the (TSP) calculated by the present model for $R_c = 4.5$ fm is shown. In Fig. 5 we compare our data to the A dependence of the (TSP) measured by Ref. 2. At 12° our results are much lower than predicted by the $A^{1/3}$ dependence, while at 22° a reasonable agreement is obtained. We believe that this difference results from the way the cross sections were extracted from the data. In Ref. 2 a linear background was taken, while in our case a (PS) background was used. This background is mainly a three-body phase space at 10° and mainly four-body at 21° . In the first case it is of a very convex shape, while in the latter it is close to a linear background in the region of interest. Should we take a linear background at 10° , our data would become substantially larger, as indicated by the open square.

C. Analysis of the (QFR) bumps

The bump clearly visible at 7° at $E_t \approx 82.5$ MeV (Fig. 2) is interpreted in terms of a quasifree reaction mechanism in which the incident ${}^3\text{He}$ interacts with the ${}^5\text{He}$ cluster of ${}^9\text{Be}$ via a charge exchange reaction leaving the α particle as a spectator. The large cross section observed is not unexpected if one takes into account that the process is actually a quasielastic one between isobaric analogues and that ${}^9\text{Be}$ has a strong α - ${}^5\text{He}$ structure. The spectrum was given by the following formula:

$$\frac{d^2\sigma}{d\Omega_t dE_t} = P \int_{\theta_{5\text{Li}}} \int_{\phi_{5\text{Li}}} R \left[\frac{d\sigma}{d\Omega} \right]_{5\text{He}({}^3\text{He},\text{t}){}^5\text{Li}} |G(\mathbf{p}_s)|^2 d\Omega_{5\text{Li}}, \quad (4)$$

where the factor P takes into account clustering probability and absorption effects (in our calculations it was a fitting parameter). R is the kinematical factor given by

$$R = \frac{1}{(2\pi\hbar)^3} \frac{(m_0 + m_T)(m_1 + m_2)}{m_T} \frac{k_i}{k_f} \left(\frac{2m_1 m_2 E_1}{m_0 E_0} \right)^{1/2} E_2 \times \left| \left[1 + \frac{m_2}{m_S} \right] E_2^{1/2} + \left[\frac{m_2}{m_S} \right]^{1/2} [(m_1 E_1)^{1/2} \cos\theta_{12} - (m_0 E_0)^{1/2} \cos\theta_2] \right|^{-1}, \quad (5)$$

where the indices 0, T , S , 1, and 2 stand for ${}^3\text{He}$, ${}^5\text{He}$, α , t , and ${}^5\text{Li}$, respectively, θ_2 is the emission angle of the triton, θ_{12} is the relative angle between particle 1 and 2, $(d\sigma/d\Omega)_{\text{He}({}^3\text{He},t){}^5\text{Li}}$ is the off-shell reaction cross section for the process ${}^5\text{He}({}^3\text{He},t){}^5\text{Li}$ (taken to be constant in our case), and $G(\mathbf{p}_\alpha)$ is the Fourier transform of the cluster wave function in ${}^9\text{Be}$:

$$G(\mathbf{p}_\alpha) = \int \chi(r) \exp(-i\mathbf{p}_\alpha \mathbf{r}) dr, \quad (6)$$

where $\chi(r)$ is the relative wave function of the ${}^5\text{He}$ and α clusters in ${}^9\text{Be}$. The Fourier transform used was of the form¹²

$$G(p_\alpha) = \left(\frac{2\pi\hbar}{\sigma} \right)^{3/2} e^{-(1/2)(p_\alpha/\sigma)^2} \quad (7)$$

with a σ parameter of 100 MeV/ c .

In the present experiment we have extracted only the shape from Eq. (4) and have normalized it to the spectrum at 7° after subtraction of (PS) and (TSP) contributions. At higher angles the presence of the (QFR) is visible but the magnitude is too small to extract meaningful information. The analysis of relevant excited states (see next paragraph) was also possible only at 7° since the cross section above that angle was too small to warrant such analysis.

D. Excited states in ${}^9\text{B}$

After stripping off the above mentioned breakup contributions, only the resonant state should remain. In Fig. 6 we show the residual spectrum obtained at 7° (the

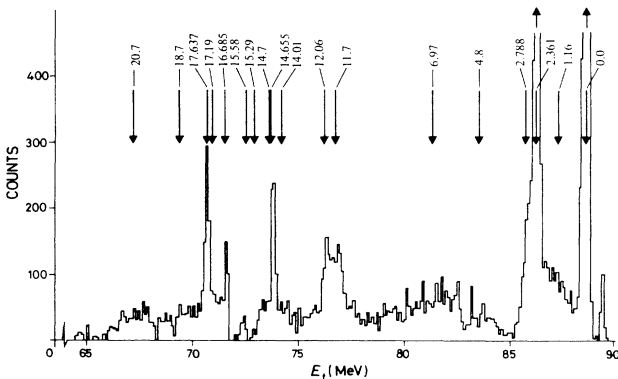


FIG. 6. Residual triton spectrum at 7° obtained after subtraction of all known continuum contributions except resonant states (heavy solid line in Fig. 2).

angle that shows most prominently the resonant states). Besides analyzing the obvious resonances, we pay special attention to the shoulder visible on the high energy side of the 2.361 MeV state since that shoulder could arise from the isobaric analog to the 1.6 MeV state in ${}^9\text{Be}$. The result in Fig. 6 is consistent with the existence of the isobaric analog states of 1.6, 4.70, and 18.6 MeV levels in ${}^9\text{Be}$.

1. $(\frac{1}{2})^+$ first excited state in ${}^9\text{B}$

In spite of numerous endeavors¹³⁻¹⁷ to measure the parameters of the ${}^9\text{B}$ state analog to the first $\frac{1}{2}^+$ $E_x = 1.68$ MeV level in ${}^9\text{Be}$, its existence has so far not been confirmed in an unambiguous way.¹ In a recent experiment, a clear indication for an excited state with parameters $E_x = 1.61 \pm 0.03$ MeV and $\Gamma = 1.0 \pm 0.2$ MeV was obtained studying the reaction ${}^9\text{Be}({}^3\text{He},t)$.¹⁸ Recently, Sherr and Bertsch¹⁹ have published an analysis of the Coulomb energy systematics indicating that the Thomas Ehrmann effect²⁰ results in a considerable lowering of the excitation energy of the isobaric analog state in ${}^9\text{B}$. Their calculation locates the level at 0.93 MeV excitation with an upper value for the width of 1.4 MeV.

In Fig. 7 we show only the high energy part of the residual triton spectrum. The present spectrum differs from the earlier published one¹⁸ that was obtained by a linear subtraction of background in the range of excitation energies from 0 to 3 MeV. In this range the dominant peaks are the ground state and the 2.36 MeV state, which, following the structure of the analog states in ${}^9\text{Be}$, have a dominant ${}^5\text{Li} + \alpha$ structure.

The state of interest in our study and the 2.78 MeV level probably have, on the other hand, a ${}^8\text{Be} + p$ structure.¹⁶ The peak structure of the residual spectrum has been analyzed in the frame of the energy dependent resonant contribution²¹

$$f(E) \approx P_c \gamma^4 / [(E - E_r)^2 + (P_c \gamma^2)^2], \quad (8)$$

where γ^2 is the reduced width of the level, E is the sum energy of the clusters interacting in a given level:

$$E = \frac{1}{2} \hbar^2 k^2 (m_A + m_B) m_A m_B \quad (9)$$

with A and B denoting the interacting clusters; k is the relative momentum of A and B ; E_r is the resonance energy above the unbound $A + B$ mass. P_c has the form

$$P_c = \frac{\rho}{A_l^2 \left[1 + \sum_{st} \gamma_{st}^2 \dot{S}_l \right]}, \quad (10)$$

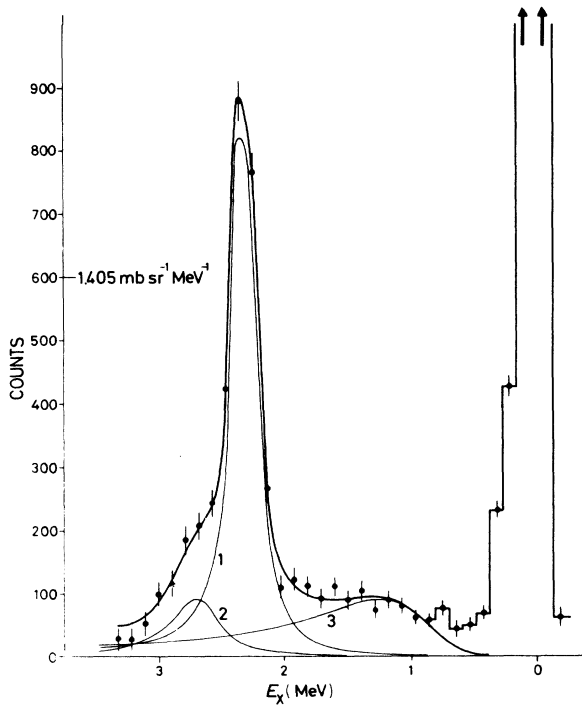


FIG. 7. The triton spectrum after subtraction of processes shown in Fig. 2 (dots with error bars) representing the peak structure in the extraction range 0–3 MeV. Curves 1, 2, and 3 are calculated line shapes for the 2.32, 2.72, and 1.16 MeV levels in ${}^9\text{B}$, respectively, and the solid line represents their sum.

where $\rho = kr$, r being the interaction radius in the p - ${}^8\text{Be}$ system taken to be 4.35 fm; A_l is the penetration factor $A_l^2 = F_l^2 + G_l^2$ (F_l and G_l are the regular and irregular solutions of the Coulomb wave function); S_l is the derivative with respect to energy of the shift function

$$S_l = \frac{\rho}{2A_l^2} \cdot \frac{dA_l^2}{d\rho} \quad (11)$$

evaluated at the energy E_r . In our case we have approximated (10) by

$$P_c = \frac{\rho}{A^2} \quad (12)$$

If this state is the $\frac{1}{2}^+$ analog, we are dealing with a proton in an $l=0$ state with respect to ${}^8\text{Be}$. The relevant values for P_c were derived from the tables of Ref. 22.

The double differential cross section has the form

$$\frac{d^2\sigma}{d\Omega_t dE_t} = \sum_i K_i f_i(E) (\text{PS}_i), \quad (13)$$

where i refers to the individual resonances, K_i is an arbitrary amplitude for each level, $f_i(E)$ is given in (8), and (PS_i) is the phase space distribution dominant for the level according to the treatment of resonant states in light nuclei proposed in Ref. 23.

In Eq. (9) A and B were taken to be α and ${}^5\text{Li}$ for the 2.35 MeV level and p and ${}^8\text{Be}$ for the $\frac{1}{2}^+$ level and the

TABLE I. Parameters of the first, second, and third excited levels in ${}^9\text{B}$ as obtained for minimum χ^2 . The γ^2 values were obtained without deconvolution for the energy resolution (~ 100 keV).

State	E_x (MeV)	γ^2 (MeV)
First	1.16 ± 0.05	1.08 ± 0.05
Second	2.32 ± 0.03	0.11 ± 0.01
Third	2.72 ± 0.04	0.22 ± 0.01

2.79 MeV level, respectively.

The results obtained are shown in Table I. The overall χ^2 for the interval of fit shown in Fig. 7 was 1.3. The line shapes resulting for each individual level from the present fit are shown in Fig. 7 (1, 2, and 3 refer to the 2.32, 2.72 and 1.16 MeV levels, respectively). The sum fit is shown with the solid line. The slightly lower position of the second and third excited state, compared with the energies quoted in the latest compilation,¹ is due to inclusion of the phase space in Eq. (13) as pointed in Ref. 23. The width of the second and third excited state are given only as fitting parameters because the data have not been deconvoluted for the energy resolution (~ 100 keV). The full width at half maximum of the $\frac{1}{2}^+$ state corresponds to (1.30 ± 0.05) MeV.

2. Other levels

Besides the known levels clearly visible in Fig. 6, we have identified possible isobaric analogs of states in ${}^9\text{Be}$ at 4.70 and 18.6 MeV, respectively. In addition, we observe a sharp strongly excited state at 16.7 ± 0.1 MeV which could be the analog of the 16.671 MeV state in ${}^9\text{Be}$, and at ~ 21 MeV we see some evidence for a broad state which could be the analog of the 20.74 MeV state in ${}^9\text{Be}$. In the literature²⁴ some data indicated a state at ~ 16.6 MeV. However, the peak was attributed to a contamination by the $({}^3\text{He}, t)$ reaction on ${}^{12}\text{C}$. In our case we have identified the peak in the whole range of

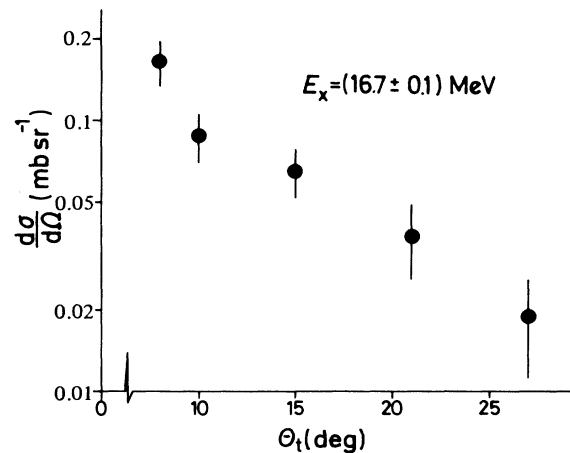


FIG. 8. Angular distribution measured for the 16.7 MeV state in ${}^9\text{B}$.

TABLE II. Parameters of hitherto uncertain or unknown levels in ${}^9\text{B}$ determined in the present work.

E_x (MeV)	Γ (MeV)
1.16 ± 0.05	1.3 ± 0.05
4.8 ± 0.03	1.5 ± 0.3
16.7 ± 0.1	< 0.1
18.6 ± 0.3	
20.7 ± 0.5	1.6 ± 0.3

our measurement from 7° to 27° and in Fig. 8 we show the angular dependence for this state.

The sharp peak in Fig. 6 at $E_1 \sim 89$ MeV is due to a leak of deuterons from the (${}^3\text{He},d$) reaction to the ground state of ${}^{10}\text{B}$. The leakage is $\sim 0.5\%$ and at all lower energies is considerably less, thus excluding any major influence of the deuteron spectra on the triton spectrum.

In Table II we show the parameters of the hitherto uncertain or unknown levels identified in the present experiment. For all the other states visible in Fig. 6, the energies and widths are consistent with those quoted in Ref. 1.

IV. CONCLUSION

The present analysis has shown how to describe the complex spectra from the (${}^3\text{He},t$) reaction on ${}^9\text{Be}$. The success in describing the continuum features made possible the extraction of residual structures. These structures have been identified as ${}^9\text{B}$ states. Some of these were hitherto unknown or uncertain.

Such treatment of complex spectra can reveal broad excited states presently lost in background. Majority of such states so far have been detected by phase shift analysis of elastic scattering data, a method that is of limited use for some states and/or nuclei.

With respect to other states of ${}^9\text{B}$, we see no evidence for the very broad $\frac{1}{2}^-$ state $E_x \sim 2.4$ MeV analog of the 2.78 MeV state in ${}^9\text{Be}$ recently calculated by Bertsch and Sherr.¹⁹ On the other hand, the result for the lowest $\frac{1}{2}^+$ level quoted here (1.16 ± 0.5 MeV) is in much better agreement with the value predicted in Ref. 19 (0.93 MeV) than the earlier estimate of Ref. 18 (1.61 ± 0.03 MeV) obtained with a linear subtraction of the background, and a Breit Wigner line shape for the resonance.

We would like to acknowledge the critical comments of Professor R. Sherr on the analysis of the parameters of the ${}^9\text{B}$ first excited state.

- ¹F. Ajzenberg-Selove, Nucl. Phys. **A413**, 1 (1984).
²O. Bousshid, H. Machner, C. Alderliesten, U. Bechstedt, A. Djalois, P. Jahn, and C. Mayer Börcke, Phys. Rev. Lett. **45**, 980 (1980).
³S. Gopal, A. Djalois, J. Bojowald, O. Bousshid, W. Oelert, N. G. Puttaswamy, P. Turek, and C. Mayer Börcke, Phys. Rev. C **23**, 2459 (1981).
⁴G. Riepe and D. Protić, IEEE Trans. Nucl. Sci. **22**, 1781 (1975).
⁵G. Paić, B. Antolković, A. Djalois, J. Bojowald, and C. Mayer Börcke, Phys. Rev. C **24**, 841 (1981).
⁶Th. Delbar, Gh. Gregoire, P. Belery, and G. Paić, Phys. Rev. C **27**, 1876 (1983).
⁷B. Antolković, G. Paić, and K. Kadija, Few Body Syst. **1**, 159 (1986).
⁸H. Ueno, T. Nakagawa, M. Baba, J. Kasagi, U. Orihara, and T. Tohei, J. Phys. Soc. Jpn. **40**, 1537 (1976).
⁹R. Serber, Phys. Rev. **72**, 1008 (1947).
¹⁰K. Kadija, Ph. D. thesis, University of Zagreb, 1985.
¹¹M. Matsuoka, A. Shimizu, K. Hosono, T. Saito, M. Kondo, H. Sakaguchi, Y. Toba, A. Goto, F. Ohtani, and N. Nakanishi, Nucl. Phys. **A311**, 173 (1978).
¹²J. R. Quinn, M. B. Epstein, S. N. Bunker, and J. M. Verba, J. Richardson, Nucl. Phys. **A181**, 440 (1972).
¹³G. D. Symons and P. B. Treacy, Phys. Lett. **2**, 175 (1962).
¹⁴E. Terranishi and B. Furubayaki, Phys. Lett. **9**, 157 (1964).
¹⁵E. F. Farrow and H. J. Kay, Phys. Lett. **11**, 50 (1964).
¹⁶J. J. Kroepft and C. P. Browne, Nucl. Phys. **A108**, 289 (1968).
¹⁷G. C. Ball and J. Cerny, Phys. Rev. **177**, 1466 (1969).
¹⁸A. Djalois, J. Bojowald, G. Paić, and B. Antolković, *Proceedings of the International Conference on Nuclear Physics, Florence, 1983* (Tipographia Compositori, Bologna, 1983), Vol. 1, p. 235.
¹⁹R. Sherr and G. Bertsch, Phys. Rev. C **32**, 1809 (1985).
²⁰J. A. Nolen, Jr. and J. P. Schiffer, Ann. Rev. Nucl. Sci. **19**, 471 (1986).
²¹U. Sennhauser *et al.*, Phys. Lett. **103B**, 409 (1981).
²²J. B. Marion, *Nuclear Data Tables* (U.S. AEC, Washington, D.C., 1960), pt. 3.
²³Th. Delbar, Gh. Gregoire, B. Antolković, and G. Paić, Phys. Rev. C **27**, 1897 (1983).
²⁴G. C. Ball and J. Cerny, Phys. Rev. **177**, 1466 (1969).